

Involute Gear Tooth Stresses Analysis Using Finite Element Modeling

Noaman Bekheet*

Associate Professor, Mechanical Engineering, University of Bahrain Isa Town, Kingdom of Bahrain P.O box 32037

Email: nbakheet@uob.edu.bh, Noaman.bekheet47@gmail.com

Abstract

The bending and surface stresses of gear tooth are major factor for failure of gear. Pitting is a surface fatigue failure due to repetitions of high contact stresses. This paper presented analysis of bending and contact stresses of involute teeth of spur gear in meshing. The involute profile of spur gear has been modeled and the simulation is carried out for analysis of stresses and deformation. 2D and 3D models are simulated. The tooth involute is designed from which the tooth is extruded to form the 3D models of spur gear. The simulation is done by finite element software package ANSYS Workbench 16.2. These stresses are also estimated using AGMA bending and contact stresses equations for comparison. The results show that the 2D model is more accurate than the 3D. Care must be taken when selecting the type of contact condition since the results are very sensitive to it. Also it is found that the elastic modulus of the material is greatly affecting the contact stresses. Poor accuracy is achieved for the bending stresses while the contact stress shows very accurate results.

Keywords: Spur gear; bending stress; contact Stress; ANSYS.

1. Introduction

Gear is one of the most critical component in a mechanical power transmission system, and most industrial rotating machinery. Spur gear is cylindrical in form and has teeth, which are of involute form in most cases [1]. A pair of spur gear teeth in action is generally subjected to two types of stresses: bending stresses and contact stress. Various research methods such as Theoretical, Numerical and Experimental have been done throughout the years.

* Corresponding author.

Theoretical and Numerical methods are primarily preferred because Experimental testing can be expensive. So many researchers have utilized FEM to predict bending stress at tooth root and contact stress at the contact point. These types of stresses may cause failures which can be minimized by careful analysis of the problem during the design stage and creating proper tooth surface profile with proper manufacturing methods. In this paper, bending and contact stresses analysis will be performed. Each gear tooth may be considering as a cantilever beam, when it transmits the load, it is subjected to bending [1, 2]. The bending stress is highest at the tooth root and can cause fatigue failure. Whereas contact stress is on the side of the tooth and may causes wear and pitting fatigue. Contact stress is a compressive stress occurring at the point of maximum Hertzian stress [1, 2]. Minimizing these stresses is helping for minimizing the transmission error and avoiding failures. The comparative analysis of ISO and AGMA standards with Finite element analysis is important for modern design and manufacturing of gears [3]. The results will allow for a better understanding of existing limitation in the current standards applied in engineering practice as well as provide a basis for future improvement of gear standard [4]. The calculation of tooth bending stress and surface durability can be enough for preliminary design or standardized purpose, but stress calculation through these simple equations given by the linear theory of elasticity and the Hertzian contact model are not good agreement with experimental results[5,13]. This stress calculation has not been studied in depth in the past. Rubin D. Chacon and his colleagues [6] and Wei Yangang [7] gives theoretical research which found location of the maximum contact stress for a pair of involute spur gear, whose contact ratio is larger than 1 and validated by finite element method. Many researcher [5, 6, 9, 11, 12] analysis the contact stress of spur gear teeth using 2D model.

They found a good agreement of AGMA contact stress with that estimated by FEM. Xianzhang Feng [8] uses a precise model in a large-scale CAD software to define the stress and displacement field for determining the maximum equivalent stress and maximum displacement. The results show good agreement between the analytical and the numerical studies. S. Sankar [10] uses circular root fillet instead of standard trochoidal root fillet in gear. He concluded that the tooth deflection in the circular root fillet is less when compared to the trochoidal root fillet. Furthermore there is appreciable decreasing in bending and contact shear stress for circular root fillet. Bharat Gupta and his colleagues [14] studied the theoretical and numerical contact stresses of spur gear. They concluded that it is necessary to develop and to determine appropriate models of contact elements to calculate contact stresses using ANSYS and compare the results with Hertzian theory. Putti Srinivasa Rao and Ch.Vamsi [15] use ANSYS and theoretical analyses of spur gear. They concluded that the exquisite feature of ANSYS enables designer to optimize the design procedure in an iterative manner based on the final plots of post-processing phase. K. G. Raptis and his colleagues [16] investigate the rating strength of spur gear using photoelasticity and FEM. They find that the deviation between the results of the applied methods falls between reasonable limits whereas it rises with increasing number of teeth of the large gear.

In the present paper, the AGMA equations of bending and contact stresses are used to validate the 2D and 3D models of mating involute teeth of spur gear using ANSYS Workbench 16.2. The effect of type of contact (bonding, frictional, frictionless, rough and no-separation) on the tooth deformation and both bending and contact stresses is studied. When using the frictional contact, friction coefficient has to be defined. The effect of the assumed friction coefficient on the result is considered. These analysis is conducted for various material properties to investigate the effect of elastic modulus.

2. Theoretical Bending and Contact Stresses

As described above, theoretical calculation of the tooth bending and contact stresses are used to validate the results of FEM.

The AGMA equation for bending stress is given by, [18]

$$\sigma_b = F_t K_o K_v K_s \frac{1}{B \times m} \frac{K_H K_B}{J} \quad (1)$$

The AGMA equation for contact stress is given by, [18]

$$\sigma_c = C_p \sqrt{F_t K_o K_v K_s \frac{K_m K_F}{B \times d_p I}} \quad (2)$$

$K_o, K_v, K_s, K_m, K_B, K_F$, are AGMA correction factors for loading condition, dynamic, size, load distribution, rim thickness, and contact surface conditions modification respectively. Since the study is static conditions, all of these factors are assumed 1 for simplicity. C_p is the material elastic constant factor calculated from the following equation:

$$C_p = \sqrt{\frac{1}{\pi \left(\frac{1 - \nu_1^2}{E_1} + \frac{1 - \nu_2^2}{E_2} \right)}} \quad (3)$$

$I = \frac{\sin \varphi \cdot \cos \varphi}{2m_N} \frac{m_G}{m_G + 1}$, m_N is the contact ratio = 1 for spur gear, m_G is the reduction ration which is 1 for equal diameter of driver and driven gears as assumed in this paper.

J is the gear geometry factor [18].

Also, Hertz theory of contact stress is used considering the contact gear teeth as cylinders with a radii equal to the involute profile radii at the contact points. The Hertz equation is given by [2].

$$\sigma_c = \sqrt{\frac{F(1 + R_1/R_2)}{R_1 B \pi \left(\frac{1 - \nu_1^2}{E_1} + \frac{1 - \nu_2^2}{E_2} \right) \sin \varphi}} \quad (4)$$

Where R_1 and R_2 are the respective radii of tooth profile curvature at the contact point. Thus

$$R_1 = R_2 = r_p \sin \varphi$$

$F = T/R_1$ is the tangential force. Other parameters are defined in Table 1.

MatLAB R13a is used to write a code for calculating the bending and contact stresses.

3. Spur Gear Geometry and Modeling

$$r_b = r_p \cos \phi$$

$$\psi = \cos^{-1}\left(\frac{r_b}{r}\right)$$

$$\theta = \tan \psi - \psi - \theta_1$$

$$\theta_1 = \tan \phi - \phi$$

$$x = -r \sin \theta$$

$$y = r \cos \theta, \quad r_b \leq r \leq r_a$$

MatLAB code has been written to calculate the involute curve coordinated x and y. The curve is then constructed using ANSYS design modeler or any CAD software. Full number of gear teeth sketch are then constructed using array command as shown in Figure 1 (b). This sketch is then extruded to form the 3D spur gear body as shown in Figure 2(a).

Using the translation command, the set of gear is constructed as shown in Figure 2 (b).

If the required model is 2D, a surface is constructed from the gear teeth sketch using the concept of the generating surface from a sketch. The thickness of the surface is then defined in mechanical modeler of ANSYS before conducting the analysis.

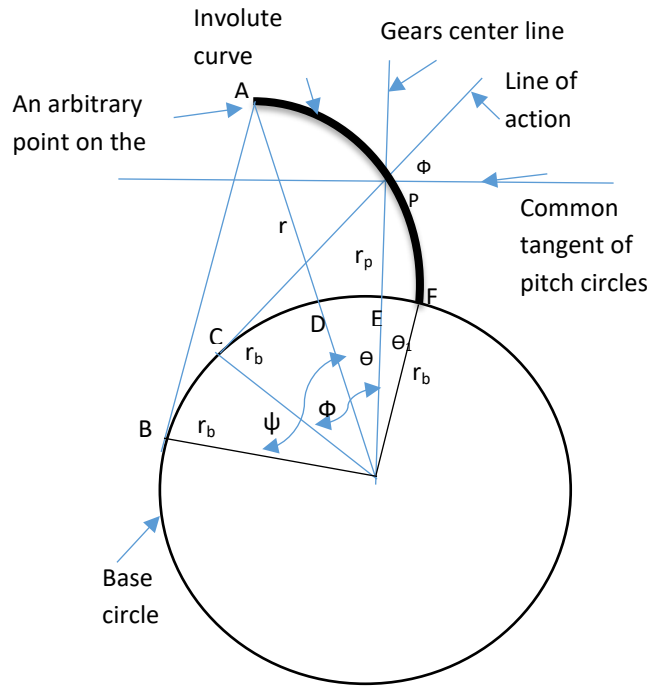


Figure 1 (a): Involute Profile

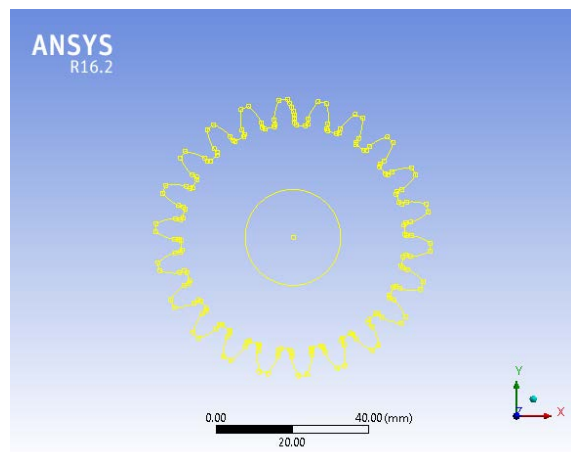


Figure 1 (b): sketch of gear teeth

To satisfy the fundamental law of gearing, tooth profile is usually cut to an involute curve [1], see Figure1 (a), which may be constructed by wrapping a string BA around a base circle, and then tracing the path APF of point A on the string. Given the gear pitch radius r_p and pressure angle Φ , the coordinates of each points on the involute curve x and y can be calculated using the following equation derived from geometry analysis [17].

The modeled spur gear dimensions and material characteristics are shown in Table 1. Different materials properties are considered to study the effect of elastic modulus on the gear tooth stresses and deformation.

The constructed gears are meshed using Tetrahedron solid element and care must be taken for the refinement process of the mesh which is affecting the results. Figure 3 (a and b) shows the meshing of the gear and mesh refinement for 3D model. Refinement must be done on 3 steps; face meshing, refinement and contact zone refinement. Refinement of level 3 and refinement of contact zone with element size of 0.4 mm are implemented. In this scenario for 3D model a number of nodes of 377909 and number of element of 256552 are achieved which are huge numbers and the CPU time is 406s. On the other hand, the 2D model is meshed and refined as shown in Figure 3 (c) with edge refinement of element size of 0.04mm. The total number of nodes is 15133 and number of elements is 4733. The CPU time is 10 s which is about 2.4% of the CPU time of 3D model.

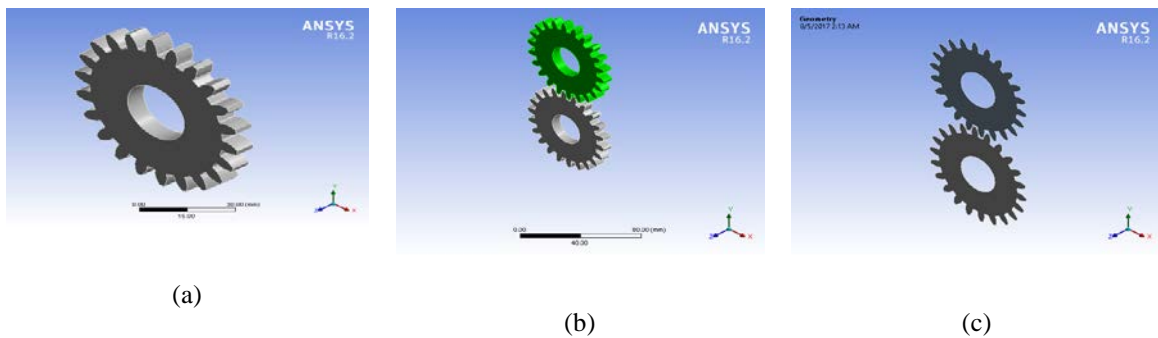


Figure 2: 3D Spur gear.

Table 1: Spur gear specification and material specifications

Descriptions	Data	Material	Elastic Modulus [GPa]	Poisson's Ratio ν
Number of teeth	22	Structure steel	200	0.3
Module	3 mm	Chromium Molybdenum	206	0.3
Pitch circle diameter $d_p=N*m$	66 mm	Alloy Steel		
Face width B	7 mm	Gray Cast Iron GG-20	91	0.25
Base circle diameter	$d_b = d_p \cos\phi$	Gray Cast Iron GG-20		
Addendum circle diameter d_2	$d_2=(N+2)*m$	Gray Cast Iron GG-30	113	0.25
Addendum a	$a=m$			
Deddendum b	$b=1.25 * m$			
Deddendum circle diameter d_4	$d_4=dp-2*b$			

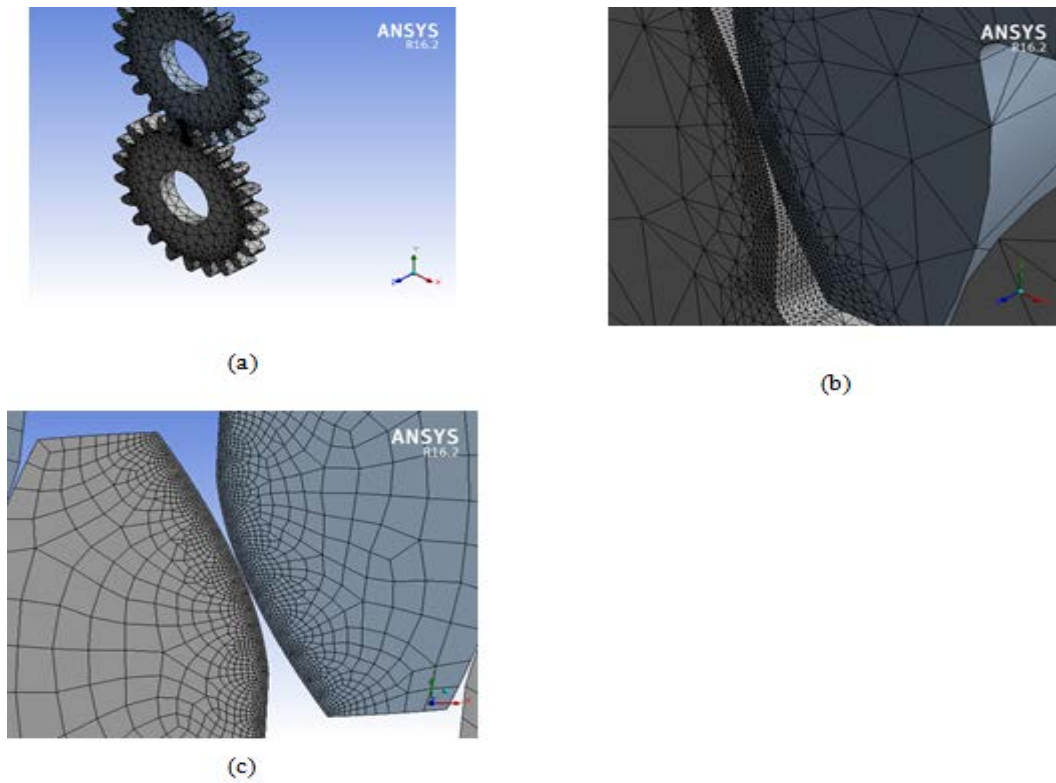


Figure 3: meshing of the modeled gear

The contact type and zone between the engaged teeth has to be defined carefully. In ANSYS, 6 contact types are available; bonded, no-separation, frictionless, rough, frictional and forced frictional sliding. The forced frictional sliding is not suitable for the current condition. The other five contact types are examined in this study. In the frictional contact type, friction coefficient of 0.15 was assumed during the analysis. A range of 0.05 to 0.3 friction coefficient is used to study its effect on the estimated stresses and deformations.

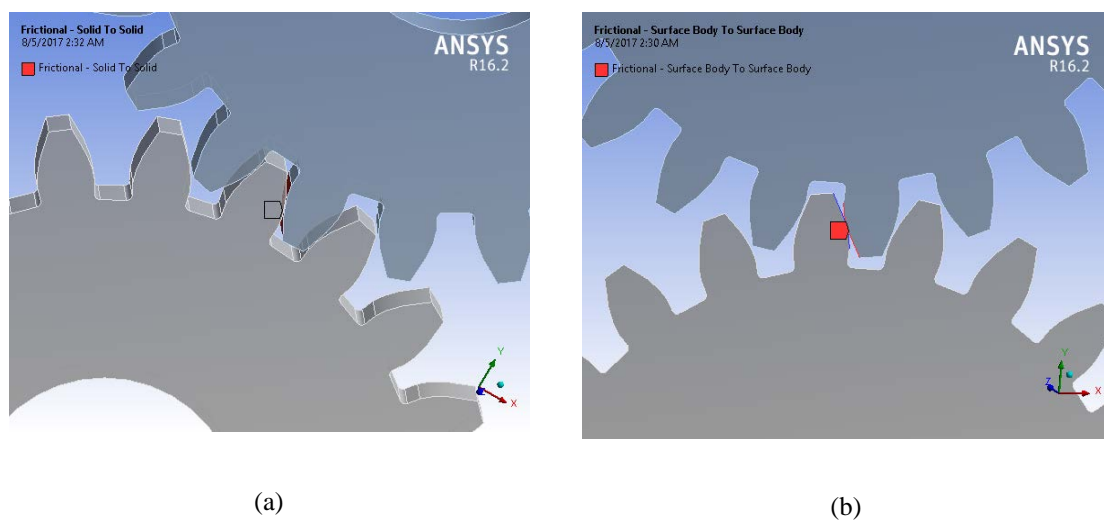


Figure 4: contact zone of the engaged teeth for: (a) 3D model, (b) 2D model

The contact type and zone between the engaged teeth has to be defined carefully. In ANSYS, 6 contact types are available; bonded, no-separation, frictionless, rough, frictional and forced frictional sliding. The forced frictional sliding is not suitable for the current condition. The other five contact types are examined in this study. In the frictional contact type, friction coefficient of 0.15 was assumed during the analysis. A range of 0.05 to 0.3 friction coefficient is used to study its effect on the estimated stresses and deformations.

Some of the very important setting of the contact conditions should be made. These are; Formulation should be Augmented Lagrange, Interface Treatment must set to Adjusted of Touch which help to define the type of contact between the selected bodies.

The boundary conditions (supports and loads) of the model must be accurately defined to avoid error of the model solution. These boundaries, Figure 5, are:

- a. Fixed support on the shaft hole of the lower gear.
- b. Frictionless support on the shaft hole of the upper gear. This allow the upper gear to rotate around its center line when the load is applied.
- c. For 3D model, 0 displacement has to be applied on one of the side face area of the upper gear.

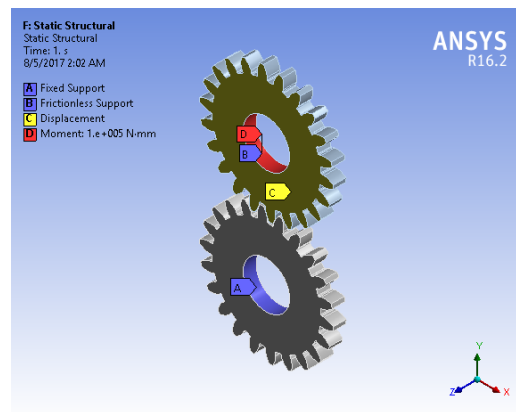


Figure 5: applied supports and load on the modeled gears

- d. The applied load is assumed to be moment around the gear center line.

A range of applied moment of 10, 20, 30, 40, 50, 60, 75 and 100 N.m is modeled to study effect of moment on stresses and deformations.

The last step before solving the model is defining of the required results. Equivalent Von Misses stresses, Principal stresses, normal stress in y direction which represents the bending stress, total deformation and contact tools. In contact tools, the status of contact and the pressure distribution on the contact area are defined. All of these results for both 3D and 2D models are presented in the following sections.

3. Theoretical Results of Bending and Contact Stresses

The results of MatLAB code for the AGMA bending and contact stresses and Hertz equation are shown in Fig. 6 for structure steel ($E= 200$ GPa and $\nu=0.3$). As shown in the figure, the contact stress calculated by AGMA equation is slightly higher than that calculated value by Hertz equation. This is due to the correction factors

introduced to AGMA equation. All other theoretical results are presented with the FEM results for comparison purpose.

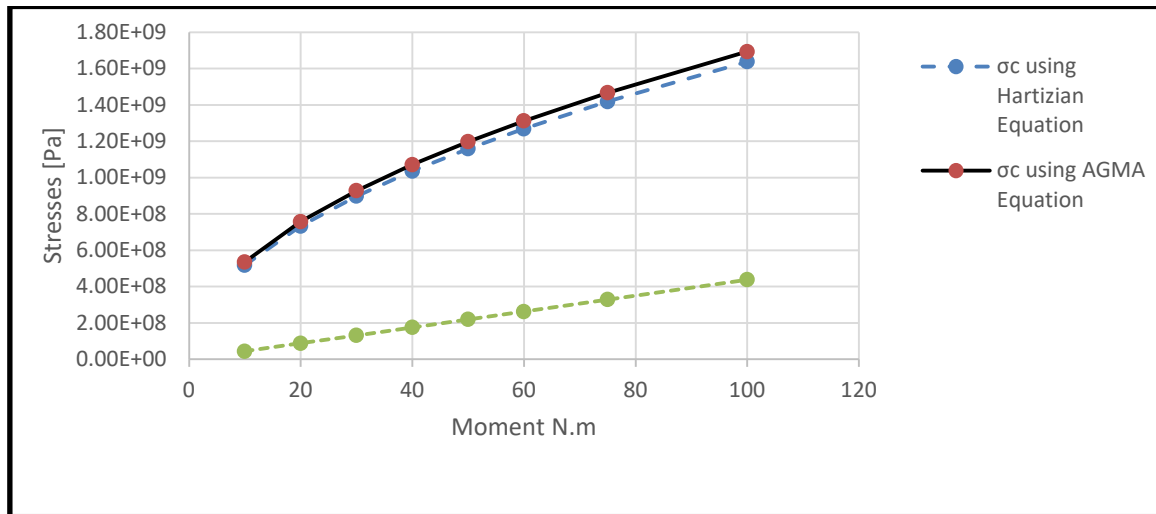
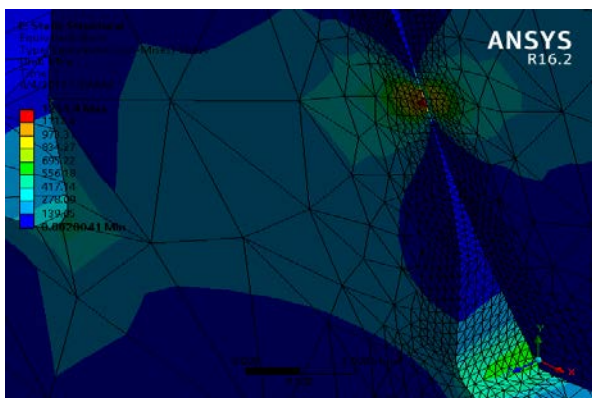


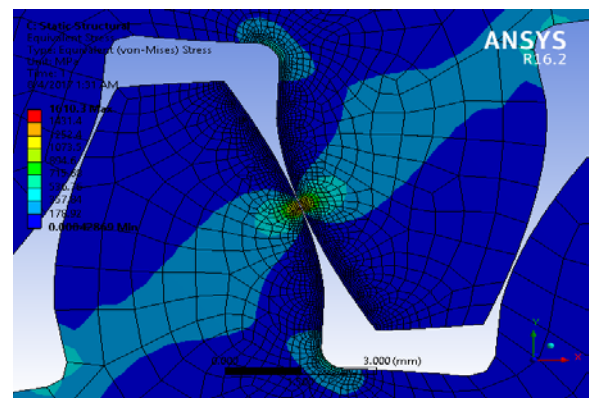
Figure 6: Variation of contact and bending stresses with moment for structure steel, E = 200 Gpa, ν=0.3

4. Results of Finite Element Model

As described above, the gear set is modeled in 2D and 3D which their results are compared with AGMA equation results. The used data are E=200 GPa, ν=0.3, moment = 100 N.m and frictional contact type with f=0.15. Maximum equivalent stress of 1251.4MPa and 1610.3 MPa obtained at the contact point for 3D and 2D models respectively as shown in Fig. 7. The large difference between the models results may be due to the size of element which it is 0.4 mm for the 3D model (377909 nodes) and 0.04 for the 2D model (15133 nodes), since the gear is also discretized in z direction for 3D model, a huge number of nodes is found. It is very expensive to decrease the element size of the 3D.



(a) 3D model: $\sigma_{eq} = 1251.4$ MPa



(b) 2D model: $\sigma_{eq} = 1610.3$ MPa

Figure 7: equivalent Von Misses stresses

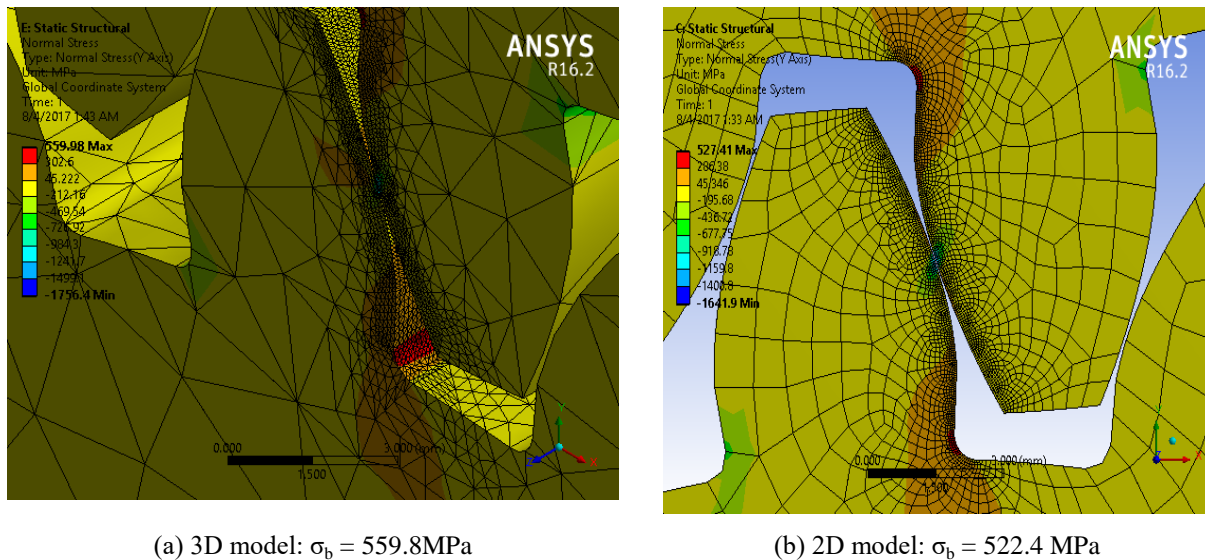


Figure 8: normal stress in Y direction (σ_b), the maximum value achieved at tooth root

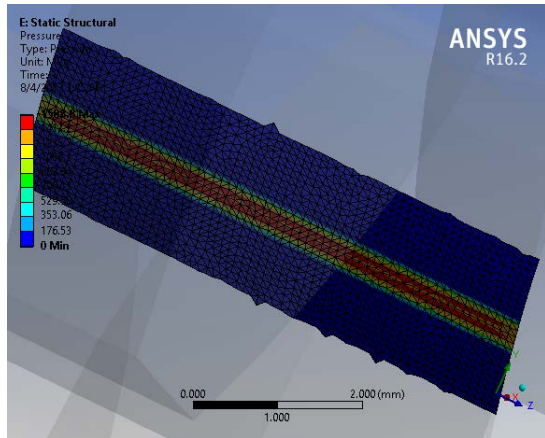
Figure 8 shows the contour of normal stress distribution on the engaged tooth for 2D and 3D models. Values of 559.8 MPa and 522.4 MPa are obtained for 3D and 2D models respectively at the root point of the tooth as seen in red color in the figure. About 6.7% difference is found. Comparing these results with the theoretical result of AGMA bending equation (437.7 MPa) the 2D model is closer result than the 3D model although the difference is about 16.5 %.

Figure 9 shows the pressure (contact stress) distribution on the contact area for both 3D and 2D models. The maximum contact stress of 1588.8 MPa and 1666.4 MPa are achieved at the middle area of the contact zone shown as red color for 3D and 2D models respectively. It is also shown in Fig. 7. Again, 4.7% difference of maximum value between the two models. Comparing these values with that obtained by Hertz and AGMA equations (1640 MPa and 1690 MPa respectively).

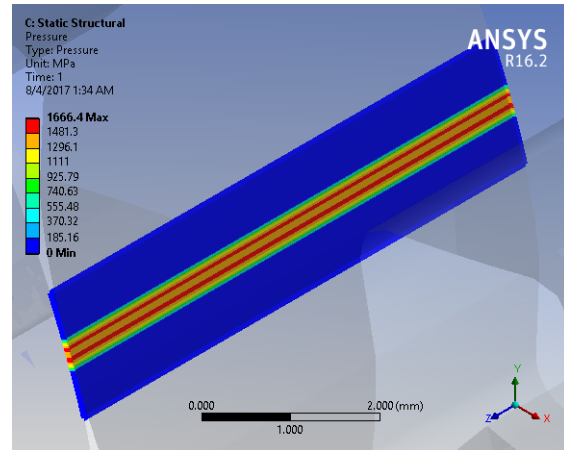
The 2D model results is in between the Hertz and AGMA equations. The AGMA equation result is 1.4% above the FEM results and Hertz equation result is 1.6% below the FEM. It can be concluded that the 2D FEM model is validated based on both Hertz equation and AGMA equation results.

Similar conclusion is made by Gupta et.al. [14]. For saving time, it is decided to use only AGMA results for the remaining comparison.

Figure 9 shows the deformation of the upper gear for both 3D and 2D models. About 2.5% difference between the results of the two models.

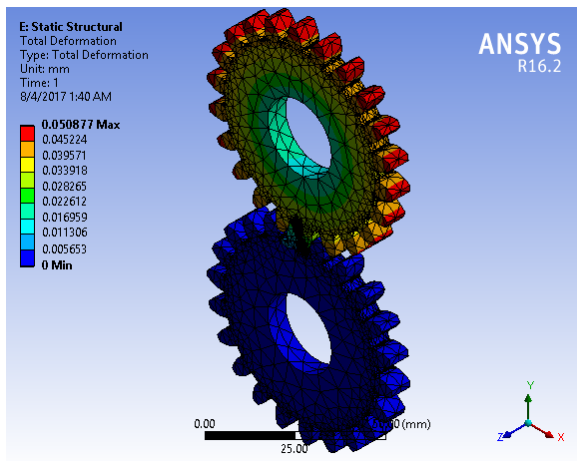


(a) 3D model: $P_{\max} = 1588.8 \text{ MPa}$

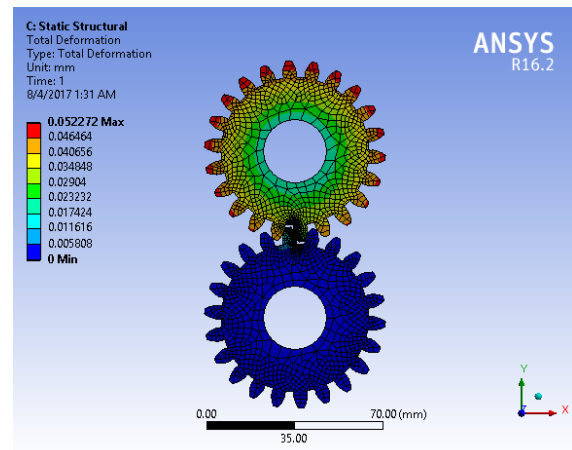


(b) 2D model: $P_{\max} = 1666.4 \text{ Mpa}$

Figure 9: pressure distribution on the contact area for (a) 3D model and (b) 2D model.



(a) 3D model: $D_{\max} = 0.0509 \text{ mm}$



(b) 2D model: $D_{\max} = 0.0523 \text{ Mpa}$

Figure 10: displacement distribution on the gear mesh for (a) 3D model and (b) 2D model

Figure 11a and 11b show a comparison between the results of FEM and AGMA equations results. For higher moment loading, the theoretical and FEM contact stresses are close with a difference of 1.7% while the bending stress show a difference of 21% as shown in Fig. 11.

A reason for this is may be the effect of deformation of the contact stress is sharing for increasing the bending stress in the FEM while AGMA equation is calculating only pure bending stress.

The difference is slightly affected by the increasing of the applied moment as shown in Fig. 12.

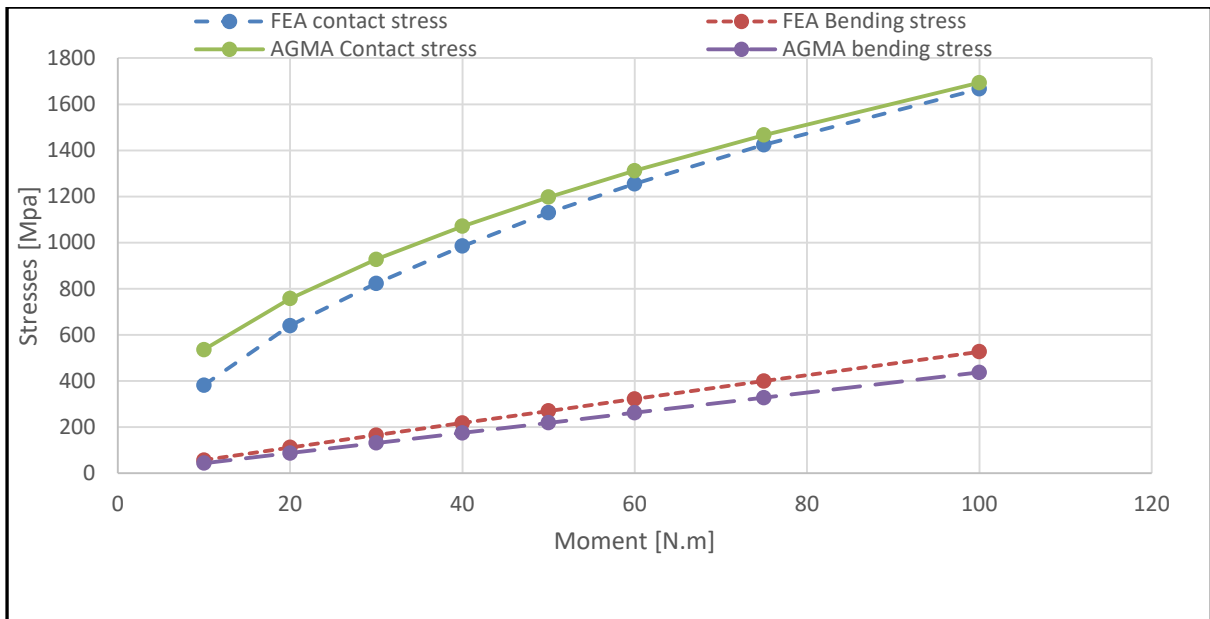


Figure 11 (a): Variation of analytical and FEA stresses for structure steel and frictional contact with $f=0.15$.

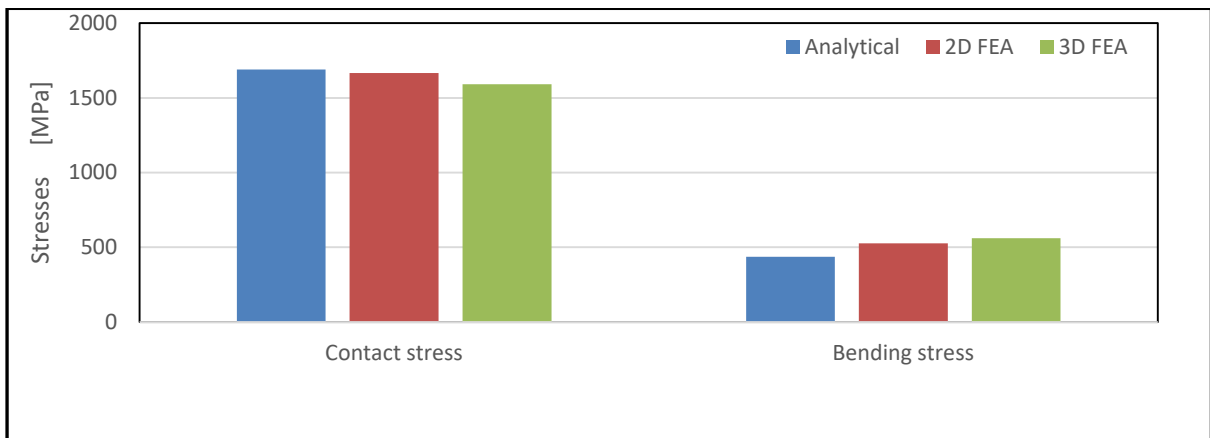


Figure 11(b): Comparison of contact and bending stresses calculated by analytical and 2D and 3D FEA

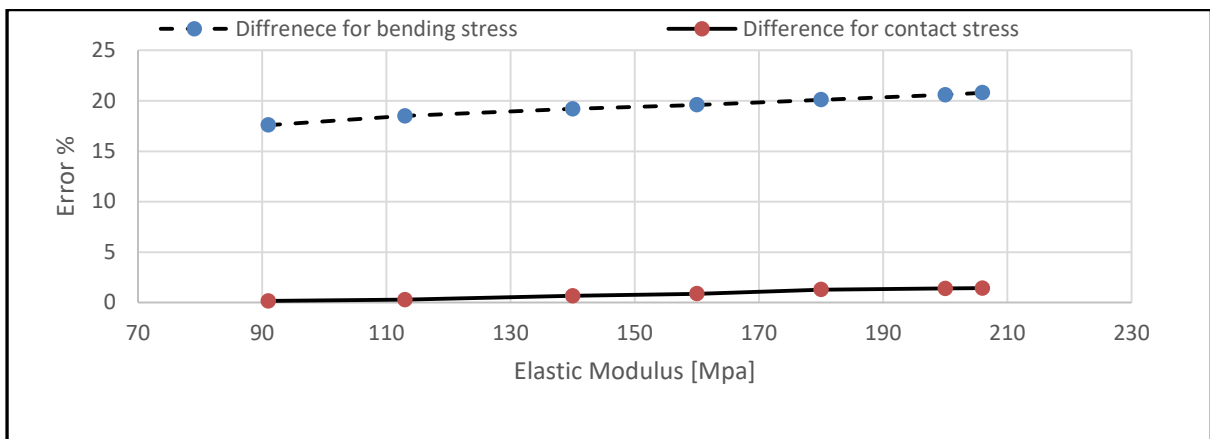


Figure 12: Error % between analytical and FEA results of contact and bending stresses

Figure 13a and 13b shows the effect of type of contact on the contact and bending stresses and the deformation for structure steel, 100 N.m moment, and $f=0.15$. Wrong results of contact stresses is obtained for bonding and no separation types while the other 3 types; frictionless, frictional and rough model give reasonable results. Similar results is obtained for the teeth deformation as shown in Figure 13b. On the other hand the bending stress is not affected by the type contact as shown in Figure13a. This may be explained as the bending stress occurs at the tooth root which is fare from the contact zone.

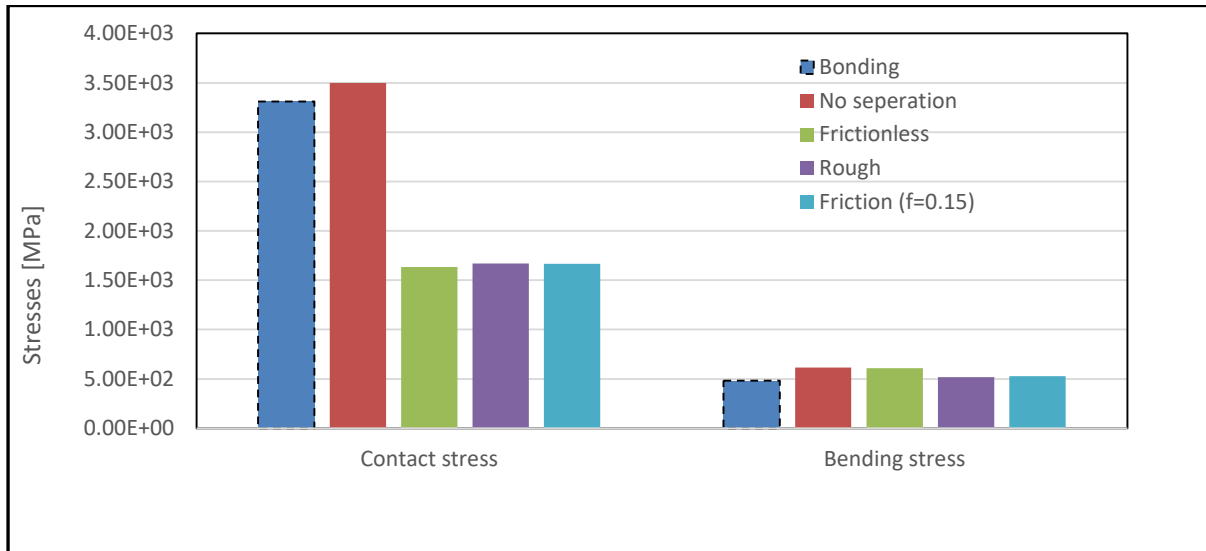


Figure 13 (a): effect of contact type on the contact and bending stresses for sturcture steel, $M = 100$ N.m

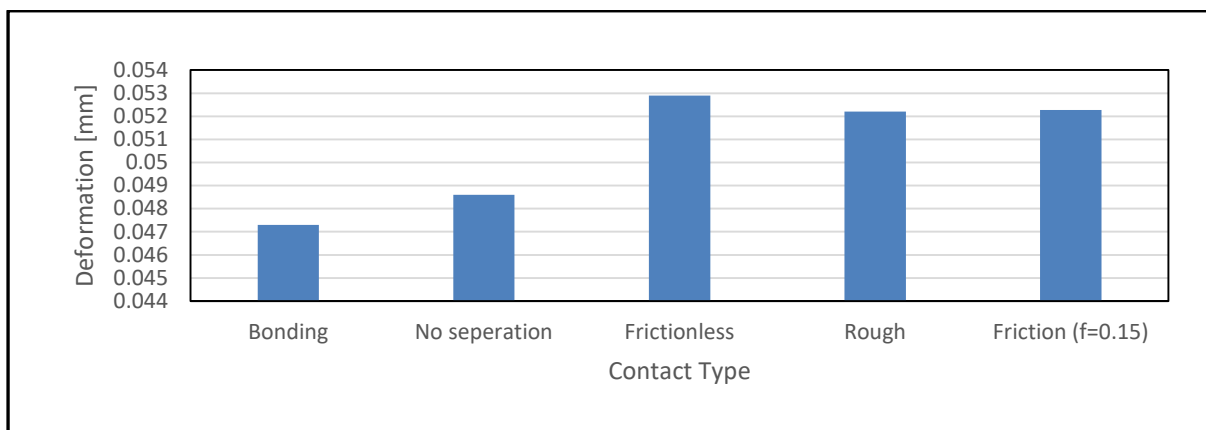


Figure 13 (b): effect of contact type on the deformation of gear

In the analysis of the frictional contact type, friction coefficient f must be defined. It is desired to investigate the effect of f on the results. Friction coefficient values of 0.05, 0.1, 0.15, 0.2, 0.25 and 0.3 are examined.

The results are shown in Figure 14 (a-c). The contact stress increases slightly up to $f = 0.2$ and then decreased for $f=0.25$ and 0.3. Bending stresses and deformation show the opposite trend.

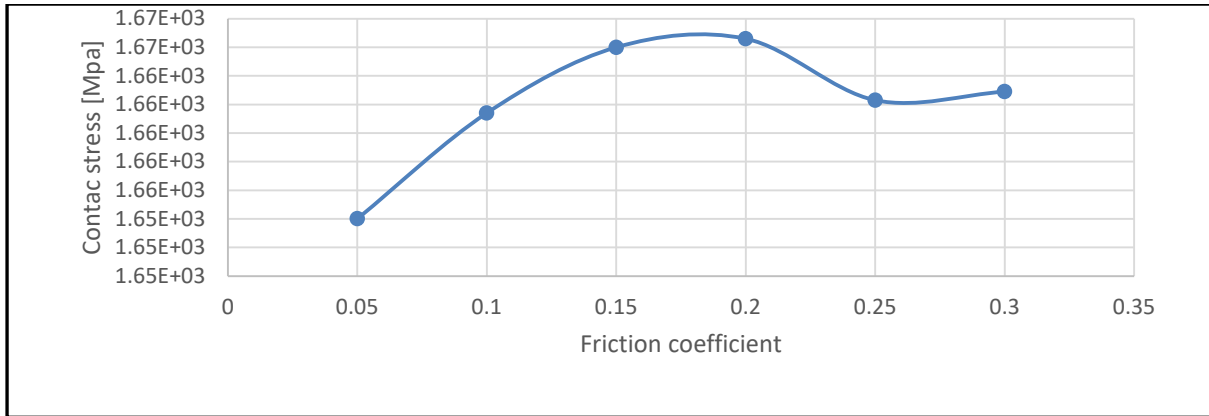


Figure 14 (a): effect of friction coefficient on contact stress

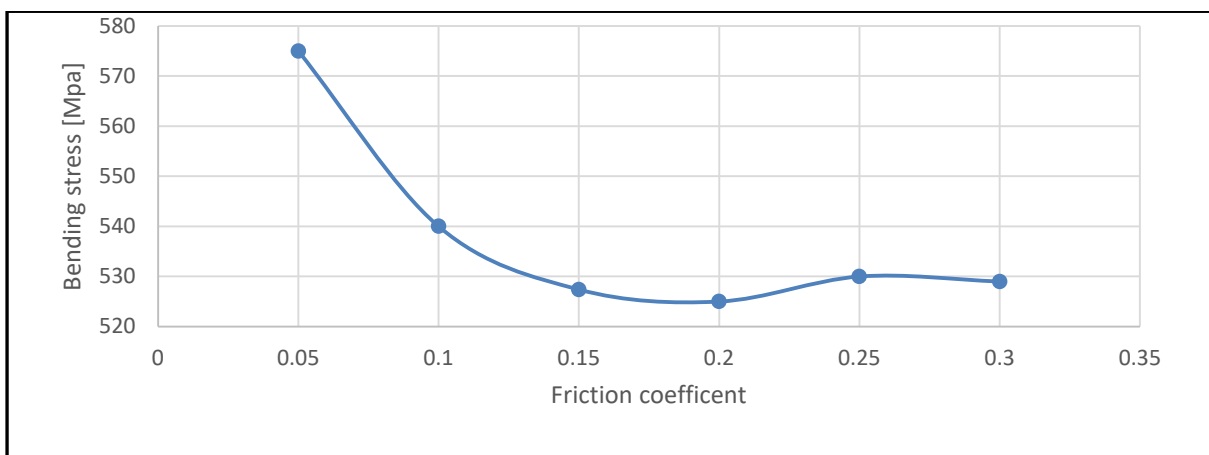


Figure 14 (b): effect of friction coefficient on bending stress

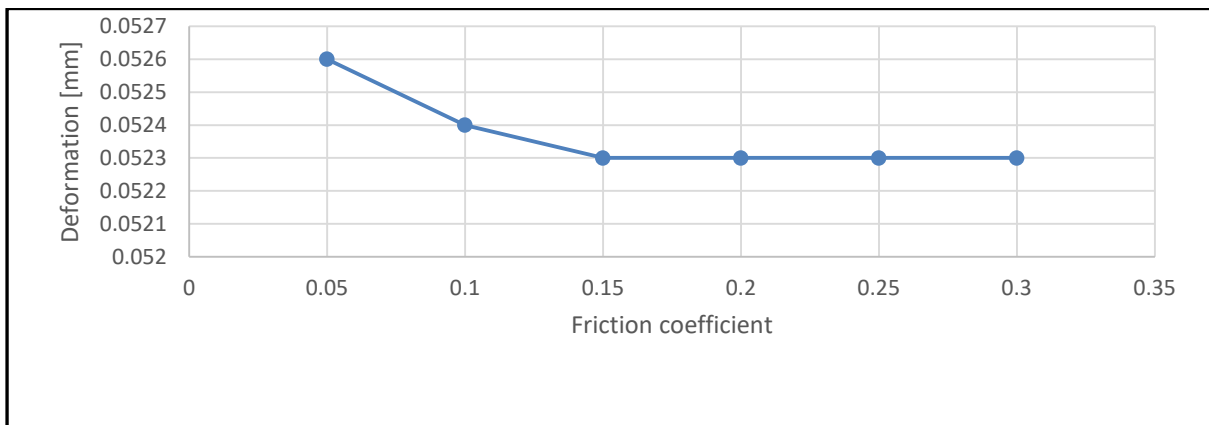


Figure 14 (c): effect of Friction coefficient on the tooth deformation for Structure steel and M=100 N.m

Finally, the effect of material properties on the contact and bending stresses and deformation is investigated. The main property considered is the elastic modulus E. A range of 91 to 206 GPa elastic modulus is used for the theoretical and numerical calculations. The results are shown in Figure 15a and 15b which indicate that bending

stress is not affected by the elastic modulus as it is expected whereas the contact stress is greatly affected by E since it is included in the deformation calculation for the contact area. As expected, also, the deformation is greatly affected by E, as E increases, the deformation decreases.

5. Conclusion

In this paper, 3D and 2D models of spur gears are developed to calculate contact and bending stresses and deformation. The results are checked with theoretical data calculated using AGMA standard. The simulation results have good agreement with the theoretical results especially the contact stress, which implies that the model is vailed. The agreement between FEM and AGMA equation for bending stresses is very poor, about 24% deviation which still need more investigation to minimize this deviation. The finite element results for different type of contact indicates that frictional contact, rough contact and frictionless contact is suitable for the current application.

In the 3D model, the results are affected by the size of the element which it is large compared with the size of element used in the 2D. This may need more study with more refinement. This will be more expensive analysis.

Extra parameters effect on the study may be considered such as module, face width, and gear center distance which need more research time.

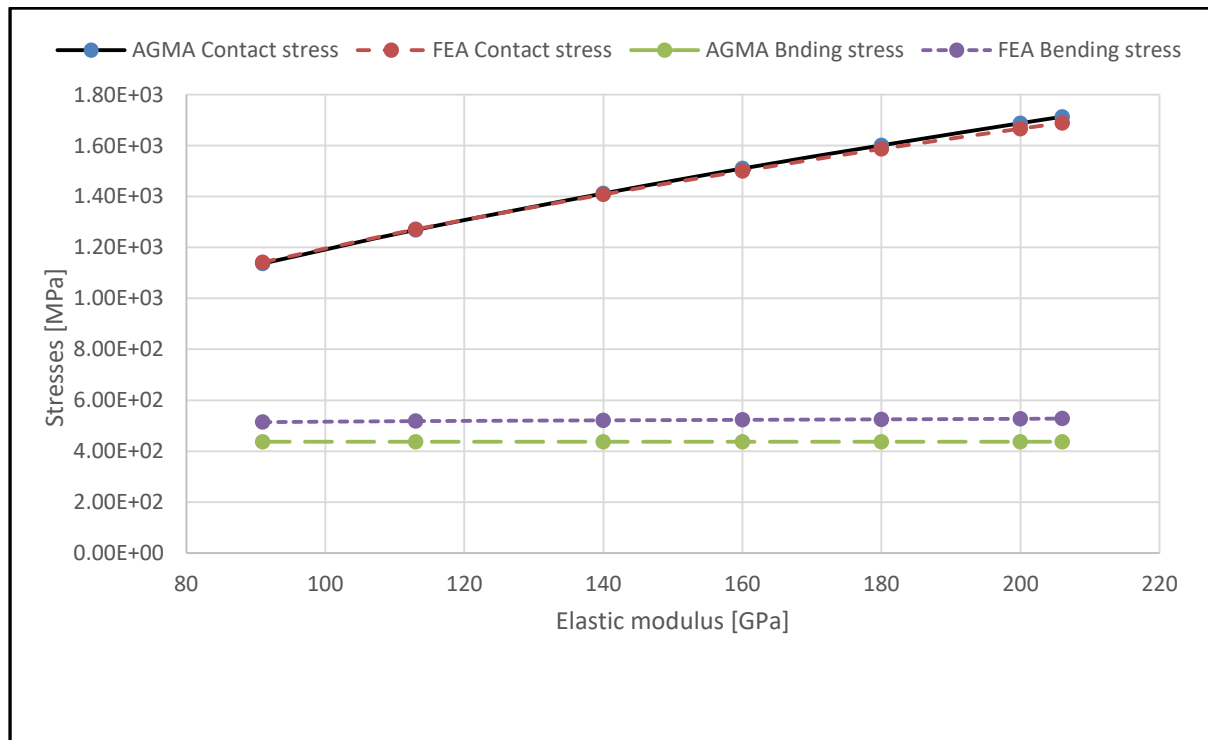


Figure 15 (a): effect of elastic modulus on the AGMA and FEA of bending and contact stresses

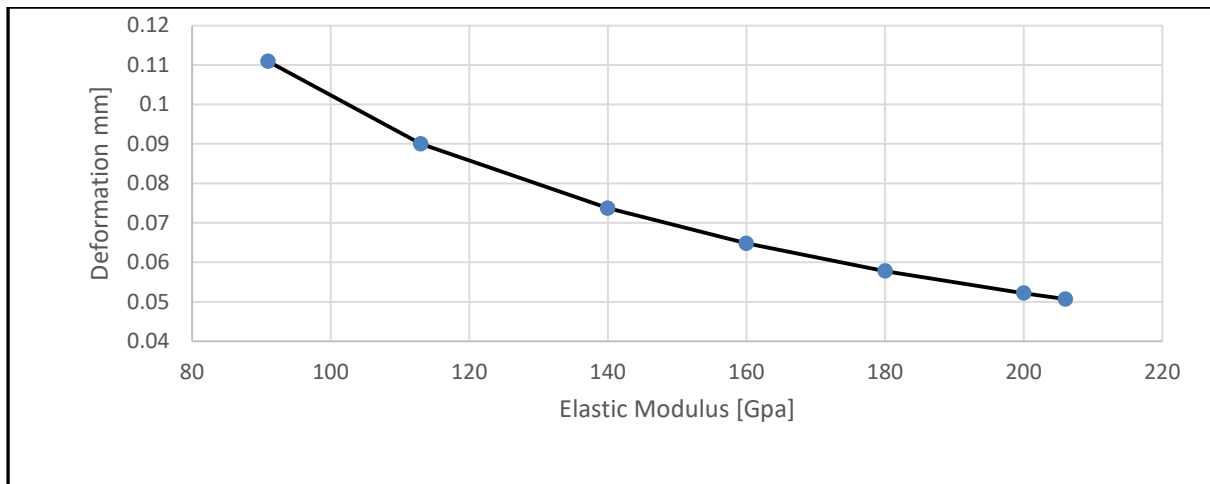


Figure 15 (b): effect of elastic modulus on the deformation of gear tooth

References

- [1]. Darle W. Dudley "Practical Gear Design" McGraw-Hill Book Company, 1954
- [2]. Peter R.N. Childs "Mechanical Design, Second edition" Elsevier Butterworth-Heinemann, 2004.
- [3]. Andrzej Kawalec, Jerzy Wiktor, Dariusz Ceglarek "Comparative Analysis of Tooth-root Strength Using ISO and AGMA Standard in Spur and Helical Gear With FEM-based Verification" Journal of mechanical Design, ASME, 2006, vol. 128/1141.
- [4]. Jose I. Pedrero, Izaskun I. Vallejo, Miguel Pleguezuelos "Calculation of Tooth Bending Strength and Surface Durability of High Transverse Contact Ratio Spur and Helical Gear Drives" Journal of mechanical Design, ASME, vol. 129-69, 2007
- [5]. Ali Raad Hassan "Contact Stress Analysis of Spur Gear Teeth Pair" WASET 58, 2009.
- [6]. Rubin D. Chacon, Luis J. Aduenza "Analysis of Stress due to Contact between Spur Gears" Wseas.us, 2010.
- [7]. Wei Yangang, Zhang Xiujuan, Liu Yankui "Theoretical research on the maximum Contact Stress of Involute spur Cylindrical Gear Pair in the External Meshing Process" IEEE, 2010.
- [8]. Xianzhang FENG "Analysis of field of Stress and Displacement in process of Meshing Gears" International Journal of Digital Content Technology and its Applications, Volume 5, Number 6, 345-357, 2011.
- [9]. Ignacio Gonzalez-Perez, Jose L. Iserte, Alfonso Fuentes "Implementation of Hertz theory and validation a Finite Element Model for stress analysis of gear drives with localized bearing contact" Mechanism and Machine Theory, Elsevier, 46,765-783, 2011.
- [10]. S. Sankar. Muthusamy Natraj, "Profile Modification- A Design approach for increasing the Tooth Strength in Spur Gear" International Journal of Advance Manufacturing Technology, Springer, 55:1-10, 2011
- [11]. Seok-Chul Hwang, Jin-hwan Lee, "Contact Stress Analysis for a pair of Mating Gears" Mathematics and computer modelling, Elsevier, 2011.
- [12]. Yogesh C. Hamand, "Analysis of Stress and Deflection of Sun Gear by Theoretical and ANSYS

- Method“ www.SciRP.org, Modern Mechanical Engineering, 1, 56-68 , 2011
- [13]. Massimiliano Pau, Bruno leban, Antonio Baldi, Francesco Ginesu “Experimental Contact pattern Analysis for a Gear-Rack system“ *Meccanica*, 47: 51-61 ,2012
- [14]. Bharat Gupta, et al.“Contact Stress Analysis of Spur Gear” *IJERT*,Vol. 1 Issue 4: 1-7 , 2012.
- [15]. Putti Srinivasa Rao and Ch.Vamsi , “Contact Stress and Shear Stress Analysis of Spur Gear Using ANSYS and Theoretical” *IJMSME*, Volume 2, Issue 2, 9-14, 2016
- [16]. K. G. Raptis, T.N. Costpoulos, G.A. Papadonoulos and A.D Tsolakis ”Rating of Spur Gear Strength Using Photoelasticity and FEM”, *American J. of Engineering and Applied Science*, 3, 1, 222-231 , 2010.
- [17]. Huei-Haung Lee ”Finite Element Simulation with Ansys Workbench 16” SDC Publications, 2015.
- [18]. Budynas-Nisbett, “Shigly’s Mechanical Engineering Design” , McGraw-Hill Primis, 2006.